TOUGHENING EPOXY COMPOSITES USING NANO- AND MICROCELLULOSE MODIFIERS

Xinying Deng[1], Anthony J. Kinloch[2], Soraia Pimenta[3], Gregory T. Schueneman[4], Stephan Sprenger[5], Ambrose C. Taylor[6] and Wern Sze Teo[7]

[1] Department of Mechanical Engineering, Imperial College London, London SW7 2AZ, UK
[1] Singapore Institute of Manufacturing Technology, Agency for Science, Technology and Research (A*STAR), 2 Fusionopolis Way, Innovis, #08-04, Singapore 138634, Singapore
Email: x.deng14@imperial.ac.uk

[2] Department of Mechanical Engineering, Imperial College London, London SW7 2AZ, UK
Email: a.kinloch@imperial.ac.uk, Web Page: http://www.imperial.ac.uk/people/a.kinloch

[3] Department of Mechanical Engineering, Imperial College London, London SW7 2AZ, UK
Email: soraia.pimenta@imperial.ac.uk, Web Page: http://www.imperial.ac.uk/people/soraia.pimenta

[4] The Forest Products Laboratory, U.S. Forest Service, Madison, WI 53726, USA
Email: gtschueneman@fs.fed.us, Web Page:
https://www.fs.fed.us/research/people/profile.php?alias=gtschueneman

[5] Evonik Nutrition & Care GmbH, Charlottenburger Straße 9, 21502 Geesthacht, Germany
Email: stephan.sprenger@evonik.com

[6] Department of Mechanical Engineering, Imperial College London, London SW7 2AZ, UK
Email: a.c.taylor@imperial.ac.uk, Web Page: http://www.imperial.ac.uk/people/a.c.taylor

[7] Singapore Institute of Manufacturing Technology, Agency for Science, Technology and Research (A*STAR), 2 Fusionopolis Way, Innovis, #08-04, Singapore 138634, Singapore
Email: wsteo@simtech.a-star.edu.sg, Web Page:
https://www.a-star.edu.sg/simtech/Research/Researcher-Portfolio/tid/176/Teo-Wern-Sze.aspx

Keywords: Cellulose, hybrid, fracture energy, glass-fibre composites, analytical modelling

Abstract

The fracture properties and toughening mechanisms of cellulose- and cellulose-rubber hybrid-modified epoxy polymers and glass-fibre (GF) composites are investigated. The cellulose modifiers used are microcrystalline cellulose (MCC) and cellulose nanocrystals (CNC), and the rubber modifiers are carboxyl-terminated butadiene-acrylonitrile (CTBN) and core-shell rubber (CSR). The toughening mechanisms of the MCC-epoxy and CNC-epoxy were identified to be crack deflection, shear band yielding, particle rupture or pull-out and debonding of the cellulose particles, which was followed by plastic void growth. An additive toughening effect is observed for the hybrid polymers. Analytical modelling of the fracture energies showed that the particle pull-out toughening contribution is negligible for CNC-epoxy, and the particle debonding and rupture toughening contributions are negligible for MCC-epoxy. The GF composites were manufactured using the wet-layup process. Cellulose modifiers did not increase the composite propagation fracture energy ($G_{C,prop}$) but slight increases in $G_{C,prop}$ occurred for the CNC hybrids. Increases in the fibre-matrix adhesion reduced the fibre toughening mechanisms in the composites that were modified with only MCC or CNC. The crack tip deformation zone is smaller than the MCC particles, reducing their toughening ability in the GF composites.

1. Introduction

The epoxy matrix of fibre composites is highly crosslinked, and thus requires toughening for use in engineering applications, e.g. by the addition of rubber particles. Nanocellulose is a promising modifier for composite materials due to its excellent properties, such as a high stiffness and crystallinity, and it has the added advantage of being derived from a sustainable source [1]. Synergistic, additive and negative toughening effects have been reported for the combination of rubber and a rigid modifier [2]. However, there are few reports on the hybrid toughening effect of combining cellulose and rubber modifiers in epoxy polymers and fibre composites.

In the present study, the fracture properties of cellulose and cellulose-rubber hybrid-modified epoxy polymers were investigated. The interlaminar fracture energies of the composites were measured and compared to the bulk fracture energy values to assess the effectiveness of the transfer of the increases in the toughness of the matrix. The toughening mechanisms of the modified polymers and composites were identified by microscopy of the fracture surfaces and of the deformation zone around the crack tip. Analytical models were used to predict the increases in toughness for the modified epoxy polymers and composites, and the predictions will be compared to the experimental results.

2. Experimental

2.1 Materials and manufacturing

The epoxy system used a stoichiometric ratio of diglycidyl ether of bisphenol A (DGEBA) epoxy resin with an epoxide equivalent weight (EEW) of 185 g/eq (Huntsman, Araldite LY556) and an accelerated methylhexahydrophtalic acid anhydride with an anhydride equivalent weight (AEW) of 170 g/eq (Evonik, Albidur HE600). The CTBN-modified resin used was a 40 wt% masterbatch in DGEBA with an EEW of 330 g/eq (Evonik, Albipox 1000). The CSR-modified resin used was a 25 wt% masterbatch in DGEBA with an EEW of 242 g/eq (Kaneka, Kane Ace® MX156). Microcrystalline cellulose (MCC) and (3-glycidyloxypropyl)trimethoxysilane (GPTMS) were purchased from Sigma Aldrich. Freeze-dried cellulose nanocrystals (CNCs) were provided by USDA Forest Service.

The cellulose modifiers were premixed with epoxy resin and GPTMS (ratio of GPTMS to modifier was 1:10, but GPTMS was not added if the cellulose modifiers were not added) before being dispersed uniformly in the epoxy resin using a three-roll mill (Exakt Technologies, Exakt 80E). For the hybrid formulations, the rubber modifiers were added into the premix with the cellulose modifiers. Three passes through the mill were used, with a front roller speed of 180 rpm, gap size of 5 μm, and roller temperature of 22°C. For the modified bulk polymers, the modified resins were mixed with HE600, degassed and cast into release-coated metal moulds. The epoxies were cured at 120 °C for 2 hours, followed by a post-cure of 160 °C for 2 hours. For the fibre composites, the modified resins were mixed with HE600, degassed and spread layer by layer onto the plain-weave glass fibre layup (Gurit, RE210D) at 50 °C. 16 layers of glass fibres were used to make a thickness of approximately 4 mm. The composites were cured at 100 °C for 2 hours, followed by a post-cure of 150 °C for 10 hours.

The MCC-epoxy is used as an example of the notation used for the epoxy formulations, see Table 1. For the GF composites, '-GF' is added behind the notation used for the epoxy polymer. For example, 'CNC10.CTBN9-GF' denotes a GF composite modified by 10 wt% CNC and 9 wt% CTBN.

Table 1. Example of the notation for the epoxy polymer formulations used in the present study.

First modifier	Concentration (wt%)	Second modifier	Concentration (wt%)	Notation used, (the number represents the wt% present)
MCC	10	-	-	MCC10
MCC	10	MX156	9	MCC10.CSRS9
MCC	10	CTBN	9	MCC10.CTBN9

2.2 Mechanical characterisation

The fracture toughness and fracture energy (K_C and G_C) were obtained from single edge notched beam (SENB) tests performed in accordance with ISO 13586 [3] (Instron, 3366), and at a rate of 1 mm/min. The sharp precrack was made by tapping a liquid nitrogen chilled razor blade into a machined notch. The yield behaviour of epoxy was analysed using plane-strain compression (PSC) tests [4]. Polished specimens of size 40 mm by 40 mm by 3 mm were loaded between 12 mm wide parallel dies at a rate of 0.1 mm/min. The results were corrected for machine and test rig compliance. The mode I interlaminar fracture energy of the composites was obtained from double cantilever beam (DCB) tests in accordance with ISO15024 [5] (Instron, 5584), and at a rate of 1 mm/min.

2.3 Imaging studies

The morphologies of the rubber modifiers in the polymers were obtained using atomic force microscopy (AFM) by scanning the microtomed surface in tapping mode, using a scanning probe microscope (Veeco, Multi-mode 8). The fracture surfaces were examined using a field-emission gun scanning electron microscope (FEGSEM) (Carl Zeiss, Sigma 300) and a SEM (Hitachi, S-3400N). The samples were coated with a 10 nm thick layer of chromium or gold to prevent charging, and an accelerating voltage of 5 kV was used. The plane-strain compression samples were loaded to just beyond the yield point and then unloaded. The unloaded samples were sectioned and polished to a thickness of 0.1 mm and were observed between crossed polarisers using an optical microscope (Zeiss, AxioScope.A1).

3. Modified epoxy polymers

A largely additive hybrid toughening effect occurs in the hybrid polymers between the MCC or CNC with the rubber modifiers, see Table 2. The toughening mechanisms observed in the epoxy polymers with only a single modifier were largely still present in the hybrids, see Figure 1. However, some of the CNC are dispersed as micro-scale agglomerates and the fracture properties of the modified epoxy polymers may improve with better dispersion. The toughening mechanisms of the MCC hybrid-modified epoxy polymers were shear band yielding, crack deflection, and particle debonding, pull-out and rupture, followed by plastic void growth. The toughening mechanisms of the CNC hybrid-modified epoxy polymers were similar to those that were identified for the MCC hybrids, except that crack deflection did not occur, since the CNC are much smaller than MCC.

Table 2. Fracture properties for unmodified and modified bulk epoxy polymers. (Mean ± SD shown.)

	K_C (MPa $m^{1/2}$)	G_C (J/m^2)		K_C (MPa $m^{1/2}$)	G_C (J/m^2)
Unmodified	0.54 ± 0.09	90 ± 29			
MCC10	1.01 ± 0.05	264 ± 27	CNC10	0.98 ± 0.05	216 ± 23
MCC10.CTBN9	1.42 ± 0.03	662 ± 29	CNC10.CTBN9	1.26 ± 0.03	535 ± 26
MCC10.CSRS9	1.40 ± 0.05	611 ± 47	CNC10.CSRS9	1.44 ± 0.04	635 ± 33

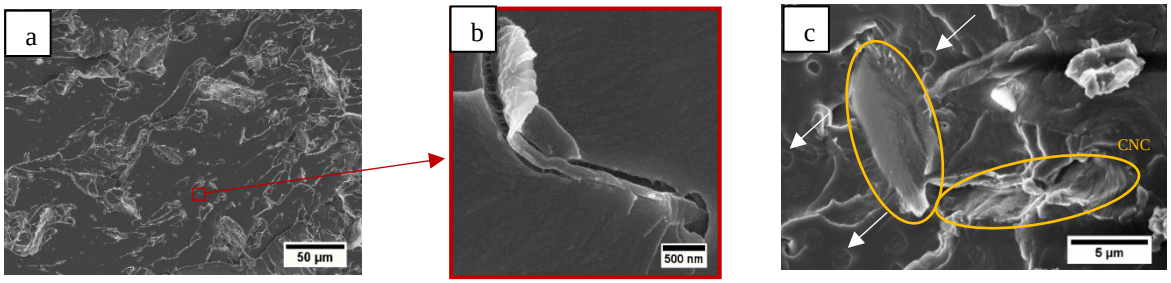

Figure 1. (a) Rough fracture surface of CNC10 and (b) a magnified view to show plastic void growth around a small pulled-out CNC, and (c) cavitated CTBN around CNC in CNC10.CTBN9. (Note: Some of the voids left behind by cavitated CTBN are highlighted with white arrows.)

The MCC- and CNC-epoxies have similar compressive stress-strain graphs, and thus only some of the compressive stress-strain graphs are shown in Figure 2. Strain softening occurs for the unmodified epoxy and the extent of strain softening decreases with the addition of modifiers. Hence, the shear bands for the cellulose-modified and hybrid-modified epoxy polymers appeared to be diffuse in nature, see Figure 3. The presence of such diffuse shear bands confirmed that shear band yielding occurred in both the cellulose-modified and hybrid-modified epoxy polymers.

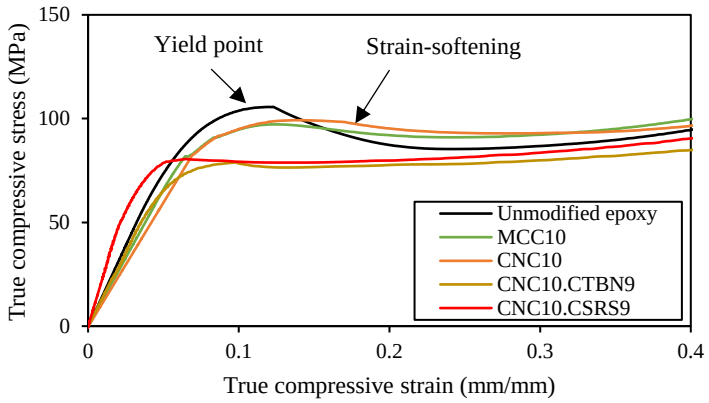

Figure 2. True compressive stress-strain graphs for the cellulose- and hybrid epoxy polymers, where the strain-softening region is indicated.

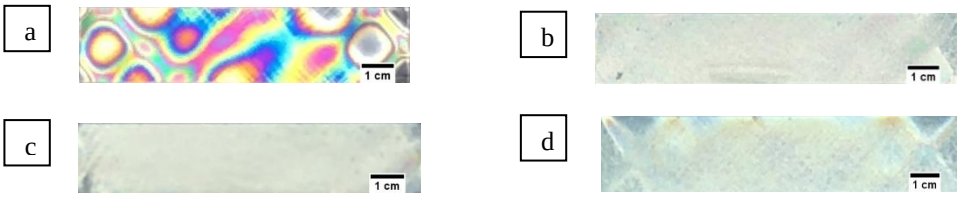

Figure 3. Crossed-polarised images of cross-section of the PSC samples that were loaded just beyond the yield point for (a) unmodified epoxy, (b) MCC10, (c) CNC10, and (d) CNC10.CSRS9.

4. Modified epoxy fibre composites

Stable crack growth and no significant R-curve effect were observed, and thus only the GF composite propagation fracture energy is discussed in the present study. The addition of MCC or CNC did not increase the fracture energy, but slight increases were found for the CNC hybrids, see Figure 4. Furthermore, toughness transfer occurred for all of the composites, which was attributed to active fibre and matrix toughening mechanisms. Broken fibres were observed on the fracture surfaces, which indicated fibre bridging and pull-out occurred, see Figure 5 (a). The matrix toughening mechanisms, such as rubber cavitation and subsequent plastic void growth, also occurred in the composites, see Figure 5(b).

The inter-fibre distance for GF was calculated to be 5.8 μm [6], and the radius of the plastic zone [7] was calculated to be between 2.3 μm and 30 μm, depending on the toughness. The fibres will restrict the plastic deformation zone, and reduce the matrix toughening ability. Hence, there was no further increase in the composite fracture energy for the composites that have a bulk G_C value greater than 535 J/m^2. This is consistent with the works of Hunston *et al.* [8], who found that the composite fracture energy will not increase further when the plastic zone size matches the inter-fibre distance, and the changeover point was found to be between 200 J/m^2 and 700 J/m^2. In addition, the toughening ability of the MCC hybrids was lower than for the CNC. The plastic deformation zone is smaller than the size of the MCC particles, limiting the toughening ability of the MCC in the GF composites.

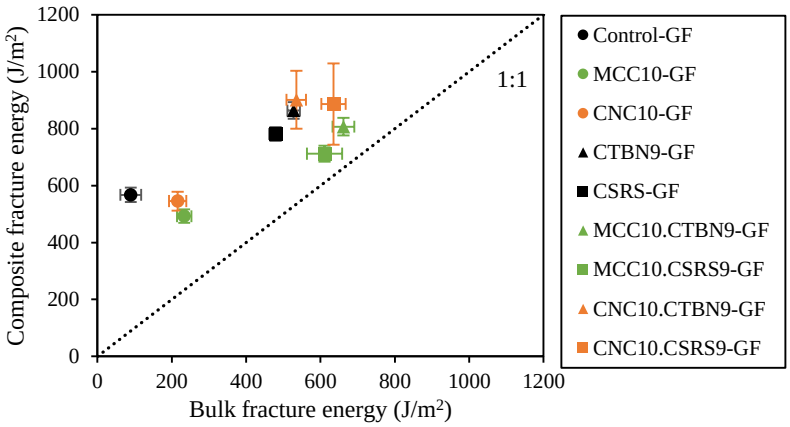

Figure 4. Composite propagation fracture energy against bulk epoxy polymer fracture energy.

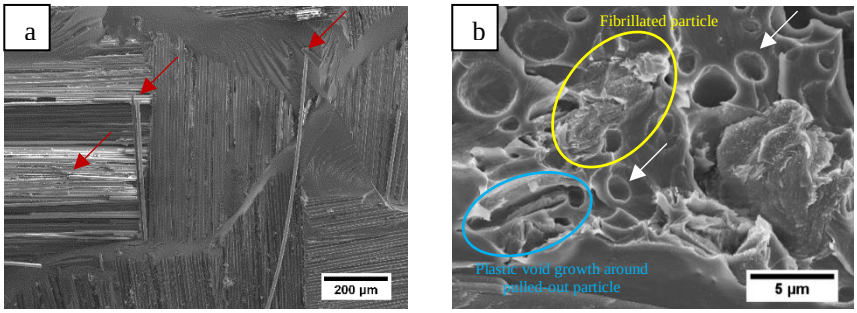

Figure 5. SEM images of fracture surface of the GF composites showing (a) broken fibres (some are highlighted using red arrows) to indicate fibre bridging and pull-out mechanism and (b) matrix toughening mechanisms, such as rubber cavitation (some are highlighted using white arrows).

5. Analytical modelling

5.1. Modelling approach

Huang and Kinloch [7] proposed a model to predict the fracture energy, G_C, of any modified epoxy polymer or composite from the sum of the fracture energy of the unmodified epoxy and the toughening contributions from the modifiers and fibres:

$$G_C = G_{CU} + \Psi_{modifiers} + \Psi_{fibres} \quad (1)$$

where G_{CU} is the fracture energy of the unmodified epoxy, $\Psi_{modifiers}$ and Ψ_{fibres} are the sum of the fracture energy contributions from the toughening mechanisms of the modifiers and fibres, respectively.

5.2 Toughening contributions from the modifiers

The value of $\Psi_{modifiers}$ is given by:

$$\Psi_{modifiers} = \Psi_{MCC/CNC} + \Psi_{CSR/CTBN} \quad (2)$$

$$\Psi_{MCC} = \Delta G_s + \Delta G_v + \Delta G_{cd} + \Delta G_{po} + \Delta G_{db} + \Delta G_r \quad (3)$$

$$\Psi_{CNC} = \Delta G_s + \Delta G_v + \Delta G_{po} + \Delta G_{db} + \Delta G_r \quad (4)$$

$$\Psi_{CTBN} \text{ or } \Psi_{CSRS} = \Delta G_s + \Delta G_v \quad (5)$$

where the fracture energy contribution ΔG_s is from shear band yielding, ΔG_v is from plastic void growth, ΔG_{cd} is from crack deflection, ΔG_{db} is from particle debonding, ΔG_{po} is from particle pull-out, and ΔG_r is from particle rupture.

ΔG_{cd} is described by the Faber and Evans model [9]. The details of ΔG_s and ΔG_v are found in [10], and ΔG_{po}, ΔG_{db}, ΔG_r are described in [11]. The fracture toughness and fracture energy of the unmodified epoxy were determined from the SENB tests to be 0.54 MPa $m^{1/2}$ and 90 J/m^2 respectively. The tensile yield strength of the unmodified epoxy was calculated from plane-strain compression tests to be 81.9 MPa [7]. The true failure strain of the unmodified epoxy (γ_{fu}) was measured to be 0.91. These values agree well with those in the literature [12]. The interfacial fracture energy and shear strength of the cellulose modifiers are taken to be 3.62 J/m^2 [13] and 16 MPa [14], respectively.

5.3 Toughening contributions from the fibres

The value of Ψ_{fibres} is given by:

$$\Psi_{fibres} = \Delta G_{Fb} + \Delta G_{Fv} \quad (6)$$

where ΔG_{Fb} is the fracture energy contribution from fibre/fibre bundle bridging and breakage, and ΔG_{Fv} is from fibre plastic void growth. ΔG_{Fb} is described by Ye and Friedrich [15] and ΔG_{Fv} is given by [7].

5.4 Predicting fracture energy for modified epoxy polymers

The properties of the cellulose particles used in the fracture energy predictions for the modified epoxy polymers are given in Table 3. The core radius and the outer radius of the CSR particles are 30 nm and 38 nm, respectively. The density of the CSR and CTBN particles are 0.910 g/cm^3 [16] and 0.948 g/cm^3 [17], respectively. The CTBN particle diameters measured from the AFM images of CTBN 9, MCC10.CTBN9 and CNC10.CTBN9 are 1.15 μm, 1.59 μm and 1.65 μm, respectively and their phase-separated volume fractions, V_f, are 6.8%, 6.3% and 6.8%, respectively.

The plastic void growth contribution was corrected by using the phase-separated CTBN V_f instead of the added V_f, as not all of the CTBN phase separates, by using the ratio of the core to the outer diameter for CSR particles, and by using the experimental void ratio of MCC and CNC measured from FEGSEM images instead of $(1+\gamma_{fu})r_p$ to calculate the volume fraction of voids.

Table 3. Properties of the cellulose modifiers used in modelling the fracture energy.

Parameter	Symbol	Unit	MCC	CNC
Length of particle	l_p	nm	20000	173
Radius of particle	r_p	nm	2500	5.8
Tensile strength of particle	σ_p	GPa	0.16 [18]	10 [18]
Young's modulus of particle	E_p	GPa	25 [19]	114 [20]
Density	ρ_p	g/cm^3	1.6 [1]	

The Faber and Evans model [9] overpredicted the crack deflection contribution, as reported by Kinloch and Taylor [21]. The extent of the contribution for the MCC10 material was calculated to be 25% of the value that was predicted by the Faber and Evans model. This value is used in the prediction for the MCC-epoxy and its hybrids. The predicted and experimental fracture energies of the hybrids are in good agreement, see Figure 6. In addition, the particle debonding and rupture contributions were found to be negligible for MCC-epoxy, and the particle pull-out contribution was negligible for CNC-epoxy.

As the MCC is larger than the CNC, less epoxy is available for the various toughening mechanisms to occur. Hence, the hybrid toughening effect for the MCC-CSR hybrid polymers is smaller than for the CNC-CSR hybrids.

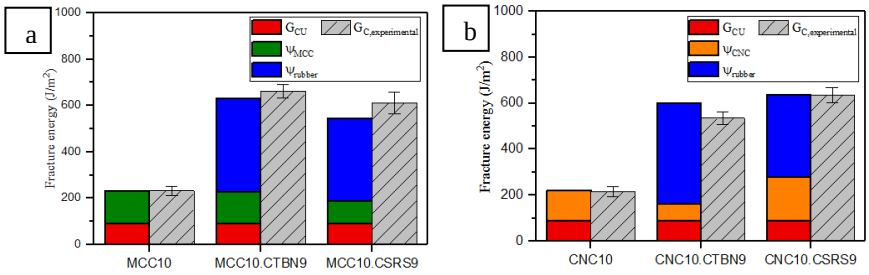

Figure 6. Predicted and measured fracture energy for (a) MCC-epoxies and (b) CNC-epoxies.

5.5. Predicting fracture energy for modified epoxy composites

The radius of the GF was measured to be 8.5 ± 1.0 μm, and its tensile strength and failure strain are 3.5 GPa and 2.5%, respectively [22]. The lengths of peeling GF and of GF at break were measured to be 0.75 to 1.4 mm, and the number of peeling GF and broken GF per unit area was measured to be 20 to 95 mm^{-2}. The fracture energy predictions generally match well with the experimental values for the GF composites, see Figure 7. The radius of the plastic deformation zone is calculated to be 8 μm for the MCC-epoxy, which will be further constrained by the stiff fibres since the fibre-spacing is calculated to be 5.8 μm. The plastic deformation zone is smaller than the MCC particles, limiting the toughening ability of the MCC in the GF composites. This resulted in an overprediction of the matrix fracture energy for the MCC-modified and hybrid-modified GF composites. In addition, the fibre contribution in the modified and hybrid composites was less than that in the unmodified-GF, which is consistent with less fibre bridging observed during DCB tests.

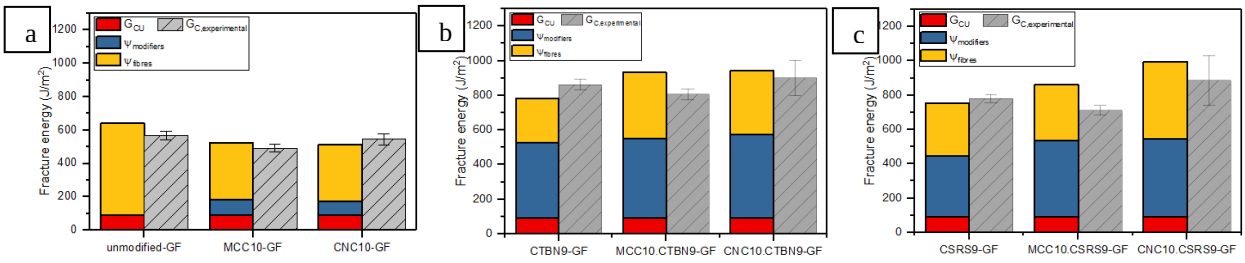

Figure 7. Predicted and measured fracture energy of the (a) epoxy GF composites modified with cellulose modifiers, and hybrid GF composites modified with cellulose and (b) CTBN, and (c) CSR.

6. Conclusions

Microcrystalline cellulose (MCC) and cellulose nanocrystals (CNC) yielded a largely additive hybrid toughening effect when added to epoxy with a rubber modifier. The toughening mechanisms observed in the epoxy polymers modified with only a single modifier were largely still present in the hybrids. However, some of the CNC are dispersed as micro-scale agglomerates and the fracture properties of the modified epoxy polymers may improve with better dispersion.The analytical predictions showed good agreement with the experimental fracture energies of the modified and hybrid polymers. The particle rupture and debonding contributions were found to be negligible for MCC-epoxy, and the particle pull-out contribution was negligible for CNC-epoxy. Hence, the main toughening contributions were due to crack deflection, particle pull-out, shear band yielding and plastic void growth for the MCC-epoxy and hybrids, and shear band yielding, plastic void growth, particle debonding and rupture for the CNC-epoxy and hybrids. Shear band yielding and plastic void growth of the rubber particles occurred for all of the hybrids.

Glass-fibre (GF) composites were fabricated via a wet-layup process. Fibre bridging, pull-out and plastic void growth were identified to be the main toughening mechanisms. The interlaminar fracture energy ($G_{C,prop}$) did not increase when MCC or CNC was added, but increased for the CNC-rubber hybrids. The analytical models largely showed good agreement with the predicted and experimental values of the mode I interlaminar fracture energy (propagation) of the modified and hybrid GF composites. The toughening ability of MCC was restricted due to the MCC particles being larger than the plastic deformation zone, resulting in an overprediction of the matrix contribution. There was also a reduction in the fibre contribution in the modified and hybrid composites as compared to the control GF composite.

Acknowledgments

The authors would like to thank Kaneka for the supply of materials, and the Agency of Science, Technology and Research (A*STAR), Singapore, for the scholarship for Ms. Xinying Deng.

References

[1] R.J. Moon, A. Martini, J. Nairn, J. Simonsen, and J. Youngblood. Cellulose nanomaterials review: structure, properties and nanocomposites. *Chemical Society Reviews*, 40 (7): 3941-3994, 2011.
[2] B.T. Marouf, Y.-W. Mai, R. Bagheri, and R.A. Pearson. Toughening of epoxy nanocomposites: nano and hybrid effects. *Polymer Reviews*, 56 (1): 70-112, 2016.
[3] ISO 13586:2000. *Plastics — Determination of fracture toughness (G_{IC} and K_{IC}) — Linear elastic fracture mechanics (LEFM) approach*. Geneva, Switzerland: ISO; 2000.
[4] J.G. Williams and H. Ford. Stress-strain relationships for some unreinforced plastics. *Journal of Mechanical Engineering Science*, 6 (4): 405-417, 1964.
[5] ISO 15024:2001. *Fibre-reinforced plastic composites — Determination of mode I interlaminar fracture toughness, G_{IC}, for unidirectionally reinforced materials*. Geneva, Switzerland: ISO; 2001.
[6] D. Hull and T. Clyne, *An introduction to composite materials*. New York, United States: Cambridge University Press;1996.
[7] Y. Huang and A.J. Kinloch. Modelling of the toughening mechanisms in rubber-modified epoxy polymers. *Journal of Materials Science*, 27 (10): 2763-2769, 1992.
[8] D. Hunston, R. Moulton, R. Moulton, N. Johnston, W. Bascom, and W. Bascom, Matrix resin effects in composite delamination: mode I fracture aspects, in *Toughened Composites, ASTM STP24372s*, N. Johnston, Editor. ASTM International: West Conshohocken, United States. 74-94. 1987.
[9] K.T. Faber and A.G. Evans. Crack deflection processes—I. Theory. *Acta Metallurgica*, 31 (4): 565-576, 1983.
[10] T.H. Hsieh, A.J. Kinloch, K. Masania, J. Sohn Lee, A.C. Taylor, and S. Sprenger. The toughness of epoxy polymers and fibre composites modified with rubber microparticles and silica nanoparticles. *Journal of Materials Science*, 45 (5): 1193-1210, 2010.
[11] R.B. Ladani, S. Wu, A.J. Kinloch, K. Ghorbani, J. Zhang, A.P. Mouritz, and C.H. Wang. Multifunctional properties of epoxy nanocomposites reinforced by aligned nanoscale carbon. *Materials & Design*, 94: 554-564, 2016.
[12] H.M. Chong. *Toughening mechanisms of block copolymer and graphene nanoplatelet modified epoxy polymers.* PhD Thesis. *Department of Mechanical Engineering.* Imperial College London. 2015.
[13] I. Siró, Y. Kusano, K. Norrman, S. Goutianos, and D. Plackett. Surface modification of nanofibrillated cellulose films by atmospheric pressure dielectric barrier discharge. *Journal of Adhesion Science and Technology*, 27 (3): 294-308, 2013.
[14] A. Asadi, M. Miller, R. Moon, and K. Kalaitzidou. Improving the interfacial and mechanical properties of short glass fiber/epoxy composites by coating the glass fibers with cellulose nanocrystals. *Express Polymer Letter*, 10 (7): 587-97, 2016.
[15] L. Ye and K. Friedrich. Mode I interlaminar fracture of co-mingled yarn based glass/polypropylene composites. *Composites Science and Technology*, 46 (2): 187-198, 1993.
[16] G. Giannakopoulos, K. Masania, and A.C. Taylor. Toughening of epoxy using core–shell particles. *Journal of Materials Science*, 46 (2): 327-338, 2011.
[17] K. Masania. *Toughening mechanisms of silica nanoparticle-modified epoxy polymers.* PhD Thesis. *Department of Mechanical Engineering.* Imperial College London. 2010.
[18] W.Y. Hamad. *Properties of cellulose nanocrystals*. *Cellulose nanocrystals*. Chicester, United Kingdom: John Wiley & Sons, Ltd; 2017. 65-137.
[19] S.J. Eichhorn and R.J. Young. The Young's modulus of a microcrystalline cellulose. *Cellulose*, 8 (3): 197-207, 2001.
[20] Y.-C. Hsieh, H. Yano, M. Nogi, and S.J. Eichhorn. An estimation of the Young's modulus of bacterial cellulose filaments. *Cellulose*, 15 (4): 507-513, 2008.
[21] A.J. Kinloch and A.C. Taylor. The mechanical properties and fracture behaviour of epoxy-inorganic micro- and nano-composites. *Journal of Materials Science*, 41 (11): 3271-3297, 2006.
[22] C. Miao and W.Y. Hamad. Cellulose reinforced polymer composites and nanocomposites: a critical review. *Cellulose*, 20 (5): 2221-2262, 2013.